

Analysis on Localization Performance for Nomadic HRIS-aided System

Yudi Jiang, Jonghyun Jeon, Jeongwan Kang and Sunwoo Kim

Department of Electronic Engineering, Hanyang University, Seoul, South Korea

{adeline, danny0418, rkdwjddhks77, remero}@hanyang.ac.kr

Abstract

In this paper, we investigate the localization problem of nomadic HRIS-aided system, focusing on a downlink scenario where a multi-antenna base station transmits multicarrier signals to a user via a Hybrid Reconfigurable Intelligent Surface (HRIS). The HRIS is equipped with a single Radio Frequency (RF) chain receiver, enabling tunable reflection and sensing through power allocation. Nomadic HRIS-aided positioning offers convenient deployment and provides reliable Non Line-of-Sight (NLoS). With such a system, we derive the Cramer-Rao lower bound (CRLB) and analysis its localization performance.

Keywords: Hybrid Reconfigurable intelligent surface; UAV; localization; CRLB

I. Introduction

In urban environments, wireless communication between ground infrastructure and ground vehicles often encounters challenges due to signal obstruction caused by tall buildings [1]. To address this issue, recent researches have proposed the utilization of Hybrid Reconfigurable Intelligent Surfaces (HRIS) equipped with Radio Frequency Chain (RFC) [2]. In this paper, by deploying HRIS on Unmanned Aerial Vehicles (UAVs) platforms, we aim to overcome the loss-of-sight (LoS) limitations commonly encountered in urban environments, offering enhanced communication capabilities in non-loss-of-sight (NLoS) scenarios [3]. We conduct a comprehensive analysis of the system performance using the Cramer-Rao Lower Bound (CRLB) framework. Through detailed simulations, we evaluate the efficacy of the nomadic HRIS-assisted system in terms of localization accuracy.

II. System Model

As shown in Fig. 1, we consider a Multiple-Input Single-Output (MISO) downlink wireless system, which consists of one M_B -antenna BS with a known location $\mathbf{p}_B = [0, 0]^T \in \mathbb{R}^2$, one UE with an unknown location $\mathbf{p}_U = [x_U, y_U]^T \in \mathbb{R}^2$, and L HRISs with unknown location $\mathbf{p}_l = [x_l, y_l]^T \in \mathbb{R}^2$, l -th represents the index of HRIS. There exists an obstacle between the BS and UE, blocking LoS path. The BS broadcasts the OFDM signal across a set of N sub-carrier's, with frequency spacing Δ_f and the frame duration $T = 1/\Delta_f$. As described in [3], the power splitting ratio of HRIS controls the proportional distribution of its reflection signal part and sensing signal part. Here we use the common power splitting factor $\rho \in [0, 1]$ to represent the percentage of sensing power at HRIS. The received signals at l -th HRIS and UE are denoted respectively as $\mathbf{y}_l \in \mathbb{C}^N$ and $\mathbf{y}_U \in \mathbb{C}^N$, which can be expressed as follows [4]:

$$\mathbf{y}_l = \sqrt{\rho P} \mathbf{d}(\tau_{BR,l}) \mathbf{c}_l^T \mathbf{a}_R(\phi_{RB,l}) \mathbf{a}_B^T(\theta_{BR,l}) \mathbf{f}_l + \mathbf{n}_{R,l}, \quad (1)$$

$$\mathbf{y}_U = \sum_{l=1}^L \sqrt{(1-\rho)P} \mathbf{d}(\tau_{BRU,l}) \mathbf{a}_B^T(\theta_{RU,l}) \text{diag}(\boldsymbol{\omega}_l) \mathbf{a}_R(\phi_{RB,l}) \mathbf{a}_B^T(\theta_{BR,l}) \mathbf{f}_l + \mathbf{n}_U, \quad (2)$$

where $\theta_{BR,l}$ represents the angle-of-departure (AOD) from the BS towards the l -th HRIS, based on the BS local

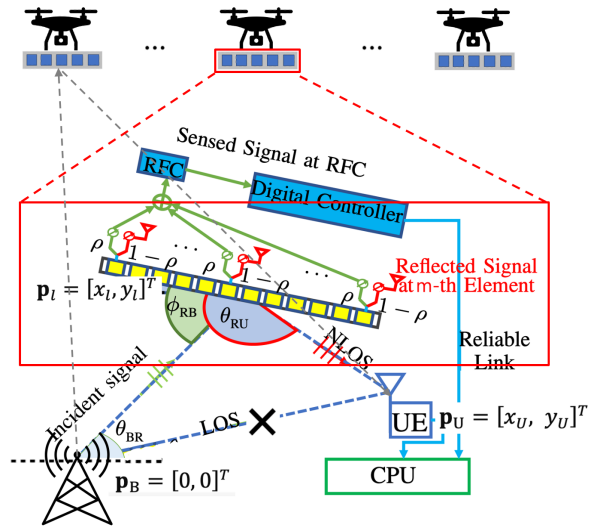


Fig. 1. Nomadic HRIS-aided System

coordinate system, $\theta_{RU,l}$ and $\phi_{RB,l}$ are the AOD from the l -th HRIS to the UE and the angle-of-arrival (AOA) to the l -th HRIS from the BS respectively, P is the BS's transmit power, $\mathbf{n}_{R,l}$ and \mathbf{n}_U represent the thermal noise following $CN(0, N_0 I_0)$. A combining vector \mathbf{c}_l^T with $|\mathbf{c}_l^T|_i| = 1$ and beamforming vector \mathbf{f}_l follow the discrete Fourier transform (DFT) codebook. The steering vectors at the BS and the HRIS are defined as follows:

$$\mathbf{a}_B(v) = \left[e^{j\frac{\pi \sin v (M_B - 1)}{2}}, \dots, 1, \dots, e^{-j\frac{\pi \sin v (M_B - 1)}{2}} \right]^T, \quad (3a)$$

$$\mathbf{a}_R(v) = \left[e^{j\frac{\pi \sin v (M_R - 1)}{2}}, \dots, 1, \dots, e^{-j\frac{\pi \sin v (M_R - 1)}{2}} \right]^T, \quad (3b)$$

where $v = \{\theta_{BR,l}, \phi_{RB,l}\}$ with M_R elements on each HRIS. The reflecting phase shift of the l -th HRIS, denoted by $\boldsymbol{\omega}_l \in \mathbb{C}^{M_R}$, is given as

$$\boldsymbol{\omega}_l = [\omega_{l,1}, \omega_{l,2}, \dots, \omega_{l,M_R}]^T, \quad (4)$$

with the m -th represents the element index of HRIS. The delay steering vector $\mathbf{d}(\tau)$ in the latter expressions is defined as [5]:

$$\mathbf{d}(\tau) = [1, e^{-j2\pi\Delta_f\tau}, \dots, e^{-j2\pi(N-1)\Delta_f\tau}]^T, \quad (5)$$

where the time of arrival (TOA) $\tau_{BR,l} = \|\mathbf{p}_B - \mathbf{p}_l\|/c$,

$\tau_{BRU,l} = \|\mathbf{p}_B - \mathbf{p}_l\|/c + \|\mathbf{p}_l - \mathbf{p}_U\|/c$ with c being the speed of light.

III. Parameters Estimation and CRLB Analysis

In this paper, we focus on the estimation of the unknown channel parameters included in the vector $\eta \triangleq [\boldsymbol{\tau}, \boldsymbol{\theta}, \boldsymbol{\phi}_{RB}]^T$,

with $\boldsymbol{\tau} = [\tau_{BR,1}, \dots, \tau_{BR,L}, \tau_{BRU,1}, \dots, \tau_{BRU,L}]^T$,
 $\boldsymbol{\theta} = [\theta_{BR,1}, \dots, \theta_{BR,L}, \theta_{RU,1}, \dots, \theta_{RU,L}]^T$ and $\boldsymbol{\phi}_{RB} = [\phi_{RB,1}, \dots, \phi_{RB,L}]$.

The CRLB is a fundamental limit on the variance of any unbiased estimator of a parameter. Here the CRLB on the unknown parameter can be written as

$$CRLB_{\eta} = \frac{1}{-\mathbb{E} \left\{ \frac{\partial}{\partial \eta} \left[\frac{\partial \ln p(\mathbf{y}; \eta)}{\partial \eta} \right] \right\}} \quad (7)$$

the Fisher Information Matrix (FIM) of η is

$$J_{\eta} = \frac{2}{N_0} \text{real} \left\{ \left(\frac{\partial \mu_n}{\partial \eta} \right)^H \left(\frac{\partial \mu_n}{\partial \eta} \right) \right\} \in \mathbb{R}^{5L \times 5L}. \quad (8)$$

The CRBs corresponding to AOAs, AODs, and TOAs can be respectively represented as follows:

$$CRLB_{\boldsymbol{\tau}} = \sqrt{[J_{\eta}^{-1}]_{1:2L, 1:2L}'} \quad (9)$$

$$CRLB_{\boldsymbol{\theta}} = \sqrt{[J_{\eta}^{-1}]_{2L+1:4L, 2L+1:4L}'} \quad (10)$$

$$CRLB_{\boldsymbol{\phi}_{RB}} = \sqrt{[J_{\eta}^{-1}]_{4L+1:5L, 4L+1:5L}'} \quad (11)$$

IV. Numerical Results and Discussions

In this section, some numerical results are presented using the simulation parameters summarized below, unless specified. The BS is located at $[0, 0]^T$ (m). With $N = 100$ subcarriers employed for transmission and reception, a carrier frequency of 28 GHz was utilized. The number of HRIS is $L=3$. The antenna spacing is set to half the carrier wavelength to minimize sidelobes, with a bandwidth of 0.2 GHz allocated for signal transmission. We set the power splitting factor $\rho=0.5$.

The results in Fig. 3. shows CRLB of estimation parameter as the number of HRIS elements change. As can be observed, with the number of HRIS elements increases, the CRLB of the channel parameters' estimation decreases. This is because when the HRIS array is larger, the reflection benefit to the sensed signal is greater and therefore the localization performance is better. We can also find out that the CRLB of ϕ_{RB} is the lowest, which is due to the fact that the estimation of ϕ_{RB} directly depends on the estimation of BS-HRIS channel parameters.

V. Conclusion

In this paper, we mount single RX-RF HRISs onto UAVs and setup a nomadic HRIS-aided system. We drive the CRLB and analyze it for the channel parameters and provide the performance simulation results of the AOA error bound, AOD error bound, and TOA error bound. For future work, we can consider extending this system to more complex and high mobility scenarios.

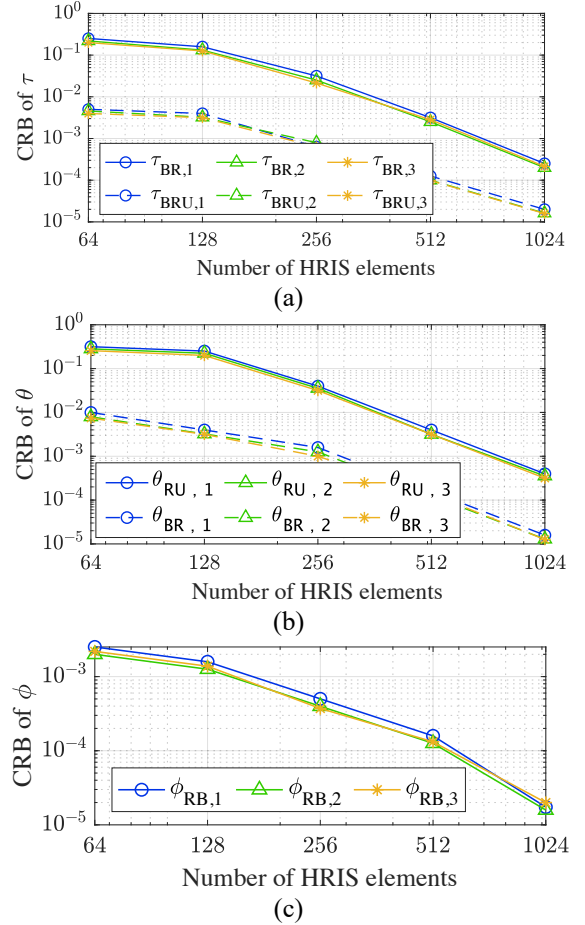


Fig. 3. CRLB vs. Number of HRIS elements

ACKNOWLEDGMENT

This work was supported by the National Research Foundation of Korea(NRF) grant funded by the Korea government(MSIT) (No. NRF-2023R1A2C3002890).

REFERENCES

- [1] Z. Zhang, et. al, "Reconfigurable Intelligent Surfaces for 6G: Nine Fundamental Issues and One Critical Problem," *Tsinghua Sci. Technol.*, vol. 28, no. 5, pp. 929–939, Oct. 2023.
- [2] G. C. Alexandropoulos, et. al, "Hybrid Reconfigurable Intelligent Metasurfaces: Enabling Simultaneous Tunable Reflections and Sensing for 6G Wireless Communications," in *IEEE Veh. Technol. Mag.*, vol. 19, no. 1, pp. 75–84, March 2024.
- [3] J. Luo, et. al, "A UAV mounted RIS aided communication and localization integration system for ground vehicles," in *2022 IEEE ICC Workshops*, Seoul, Korea, Republic of: IEEE, May 2022, pp. 139–144.
- [4] R. Ghazalian, et. al, "Joint User Localization and Location Calibration of a Hybrid Reconfigurable Intelligent Surface," *IEEE Trans. Veh. Technol.*, vol. 73, no. 1, pp. 1435–1440, Jan. 2024.
- [5] J. Kang, et. al, "Signal Classification with Linear Phase Modulation for RIS-Assisted Near-Field Localization," in *GLOBECOM 2022*, Rio de Janeiro, Brazil: IEEE, Dec. 2022, pp. 4013–4019.